Embedding oxygen heterocycle into BODIPY to enhance intersystem crossing for photodynamic therapy

Yu Zhang,[a,†] Zhiqiang Cui,[b,†] Jakub Širůček,[c,d] Denis Jacquemin,[*,c,e] Boris Le Guennic,[*,d] Xiaohong Sun,[b*] Xin-Dong Jiang[a*] and Gaowu Qin[a]

[a]Institute for Strategic Materials and Components, Liaoning & Shenyang Key Laboratory of Functional Dye and Pigment, Shenyang University of Chemical Technology, Shenyang, 110142, China. E-mail: xdjiang@syuct.edu.cn

[b]Department of Neurology, the Fourth Affiliated Hospital of China Medical University, Shenyang, 110032, China. Email: xhsun@cmu.edu.cn

[c]Nantes Université, CNRS, CEISAM UMR 6230, F-44000 Nantes, France. E-mail: Denis.Jacquemin@univ-nantes.fr

[d]Univ Rennes, CNRS, ISCR (Institut des Sciences Chimiques de Rennes) UMR 6226, F-35042 Rennes, France. E-mail: Boris.Leguennic@univ-rennes.fr

[e]Institut Universitaire de France (IUF), F-75005 Paris, France.

[†]These authors contributed equally to this work.

1. Experiment

2. Synthesis

3. NMR

4. HRMS

5. Table and Figure

6. X-ray data

7. Checkcif

1. Experiment

1.1 General

Unless otherwise noted, all chemical reagents and organic solvents were of analytical quality and obtained from Energy Chemical & Technology (Shanghai) Co. Ltd. without extra purification. A VARIAN Mercury 500 MHz spectrometer has been employed to record ^{1}H NMR spectra. Determined ^{1}H NMR chemical shifts (δ) from Me_4Si are presented in ppm downfield by trace amounts of chloroform (7.26 ppm). On a VARIAN Mercury 125 MHz spectrometer, ^{13}C NMR spectra were obtained in $CDCl_3$, reporting in ppm with the internal chloroform signal at δ = 77.0 ppm as the reference. The precise molecular weight of the product was determined using a high resolution mass spectrometer. At 298 K, an absorption spectrogram was taken using a UV-2550 spectrophotometer. Utilizing an F-128 spectrophotometer, fluorescence spectra have been recorded and displayed as cm^{-1}. The F-98 spectrophotometer was used for measuring the absolute fluorescence quantum yield. A temperature-measuring camera maintains record of the solution temperatures. A fiber connected laser system was implemented to control a 915 nm laser, which was deployed as the light source for the light irradiation and was bought from Changchun New Industries Optoelectronics Technology. A CEL-NP 2000 power meter was used to test the optical power density, it was bought from Beijing Zhong Jiao Jin Yuan Technology Co, Ltd. The CCK8 assay was via BioTek Synergy H1 microplate reader. To estimate fluorescence visualization, a Confocal Laser Fluorescence Microscope FV1200 (Olympus, Japan) was employed.

1.2 Computational method

All calculations have been performed by using the Gaussian 09 programs. The geometry was optimized by B3LYP/6-31+g**, and the electronic structure analysis was obtained from TD-B3LYP/TZVP.

1.3 Singlet oxygen detection

Utilizing 1,3-diphenylisobenzofuran (DPBF), the $^{1}O_2$ production in toluene was determined. The absorbance of DPBF at 416 nm was adjusted to about 1.5 in toluene

and the absorbance of dye molecule was adjusted to about 0.8. The characteristic absorption of DPBF was applied to characterize $^1O_2$ production. The absorption value of the dye molecule indicates the photo-stability of the dye. A 635 nm, 690 nm or 808 nm laser light source is used, the optical radiation power is 0.1 W/cm^2, and the illuminated time is 0-17 min.

The $^1O_2$ production efficiency of the dyes can be calculated by the following formula under the reference of methylene blue (MB) with known $^1O_2$ production rate efficiency (57% in DCM solution).

$$\Phi_{sam} = \Phi_{MB}(\frac{m_{sam}}{m_{MB}})(\frac{F_{MB}}{F_{sam}})$$

Where "sam" represents the unknown dye molecule and "MB" represents the reference methylene blue. "m" is the slope of DPBF absorption peak decline, "F" is the absorption correction factor, F = 1-10$^{-O.D.}$. O.D. represents the absorption value of the sample at the wavelength of light radiation.

1.4 Calculation of photothermal efficiency

The photothermal conversion efficiencies (η) was calculated using the following method:

$$\eta = \frac{hs(T_{Max} - T_{Surr}) - Q_{Dis}}{I(1 - 10^{-A})}$$

h means heat transfer coefficient, *s* was for container surface area, Q_{Dis} stands for heat dispersed from the laser via the solvent and container, *I* was for laser power, and *A* represents for absorbance at excitation wavelength. η denotes photothermal conversion efficiency.

$$hs = \frac{mC}{\tau_s}$$

m is the total quantity of the photothermal reagent containing solution, *C* represents the temperature coefficient, and τ_s is the relevant time constant.

$$t = -\tau_s \ln(\theta)$$

The temperature of the driving force is a non-dimensional parameter termed θ.

$$\theta = \frac{T - T_{Surr}}{T_{Max} - T_{Surr}}$$

T is the current temperature, T_{Max} is the highest steady state temperature, and T_{surr} denotes the surrounding temperature.

1.5 Cell Counting Kit 8 assay

The HEPG2, LN229 and MCF-7 were cultured in 96-well plates for 24 h respectively and treated with various concentrations of OhR-BDP NPs with or without 808 nm laser irradiation. Cell viability was assessed using CCK8 reagent after 2 h of cultivation, and absorbance at 450 nm was measured using a microplate reader (BioTek, USA).

1.6 Cell grouping

LN229 cells were divided into four groups: Control group, NPs group, Light group, Light+NPs group. Cells from the Control group were untreated. Cells from the NPs group were treated with 20 μM NPs for 24 h. Cells from the Light group were only irradiated by 808 nm NIR laser for 10 min. Cells from the Light+NPs group were treated with 20 μM NPs for 24 h and then irradiated by 808 nm NIR laser for 10 min.

1.7 JC-1 stanning

The JC-1 assay kit was used to measure mitochondrial membrane potential in four groups of LN229. The cells were stained with JC-1 dye and JC-1 monomer with green fluorescence and JC-1 aggregate with red fluorescence were visualized by fluorescence microscopy (Zeiss, Germany).

1.8 Intracellular ROS level

Intracellular ROS levels were measured using the ROS Assay Kit (Servicebio, China). Four groups of cells were incubated with DCFH-DA probe at 37 ℃ for 30 min in the dark. Images of the cells were taken using an inverted fluorescence microscope (Zeiss, Germany).

1.9 Flow cytometry assay

LN229 from four groups were assessed for apoptosis using Annexin V-PE/7-AAD Cell Apoptosis Detection Kit (Servicebio, China). Cells were stained with Annexin V-PE and 7-AAD, then analyzed using flow cytometry (BD, USA).

1.10 Animals Grouping and Treatments

LN229 were injected subcutaneously into the nude mice to establish xenograft nude mouse model. When subcutaneous tumor volume reached 300 mm^3, the tumor-bearing nude mice were randomly divided into four groups (3 mice per group). Mice from Control group were untreated; Mice from the NPs group were injected with 100 μL 20 μM NPs via the tail veins. Mice from the Light group were only treated by the irradiation of 808 nm NIR laser at subcutaneous tumors for 10 min. Mice from the Light + NPs group were firstly injected with 100 μL 20 μM NPs via the tail veins and then subcutaneous tumors were irradiated by 808 nm NIR laser for 10 min at 24 h post injection. Tumors were harvested 3 days after treatment. The volume and weight of tumors were measured and recorded.

1.11 Immunohistochemistry

To analyze ki67 protein expression, tissue sections were deparaffinized and treated with antigen retrieval buffer. Endogenous peroxidase was blocked with H_2O_2, and sections were incubated with ki-67 antibody (Servicebio, China) overnight and secondary antibodies for 1 h. After incubating with DAB chromogenic solution for 5 min, the nuclei were stained with hematoxylin. The sections were dehydrated, sealed, and scanned under the slide scanner.

1.12 TUNEL staining

TUNEL staining (Servicebio，China) was used to detect apoptosis in tissue sections from four groups of mice. Sections were incubated with a mixture of TDT enzyme, dUTP, and buffer, then sealed with anti-fluorescence quencher

with DAPI. Expression levels of TUNEL were observed under a confocal microscope (Nikon AXR, Japan).

1.13 Transmission electron microscopy (TEM)

Four groups of subcutaneous tumorswere fixed for 2 h in a transmission electron microscopy (TEM)-specific fix solution and then washed twice in PBS. Osmic acid was used to stain the tissues, and alcohol and acetone were used to dehydrate the samples. The cells were embedded in resin and then stained with acetic acid uranium and lead before being examined by TEM (Hitachi Co., Tokyo, Japan).

2 Synthesis

2.1 Synthesis of 8-methoxy-3-phenyl-1,4,5,5a-tetrahydrochromeno[2,3-g] indole

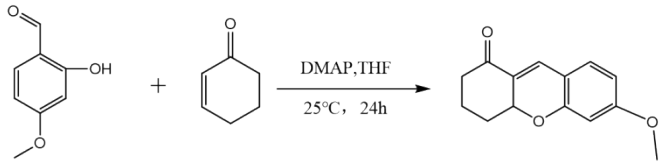

Under N_2, 2-hydroxy-4-methoxybenzaldehyde (2.0 g, 13.14 mmol) and 2-cyclohexane-1-one (1.26 g, 13.14 mmol) were added to 30 mL THF in presence of 4-dimethylaminopyridine DMAP (0.8 g, 6.57 mmol). The mixture was stirred for 24 h at r.t. The mixture was extracted with CH_2Cl_2 (2 x 40 ml) and the organic layer was washed with brine (2 x 40 ml) and dried with anhydrous Na_2SO_4. The solvent was removed by evaporation and separated by column chromatography (CH_2Cl_2/*n*-hexane = 1:1) to give 6-methoxy-2,3,4,4a-tetrahydro-1H-xanthen-1-one-ketone (2.42 g, 10.51 mmol, 80%) as a reddish brown crystalline compound. ^{1}H NMR (400 MHz, $CDCl_3$): δ (ppm) 7.42 (d, ^3J = 2.0 Hz, 1H), 7.13 (t, ^3J = 10.0 Hz, 1H), 6.51 (dd, ^3J =8.4 Hz, ^4J =2.4 Hz, 1H), 6.43 (d, ^4J =2.4 Hz, 1H), 4.94-4.98 (m, 1H), 3.79 (s, 3H), 2.51-2.57 (m, 1H), 2.44-2.49 (m, 1H), 2.33-2.41 (m, 1H), 2.03-2.09 (m, 1H), 1.93-2.01 (m, 1H), 1.64-1.74 (m, 1H).

2.2 Synthesis of pyrrole

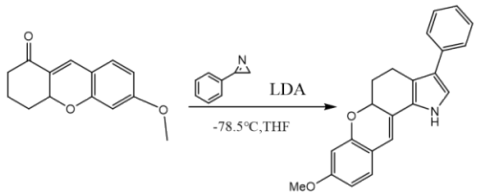

Under N_2, LDA (10.5 mmol) in THF (10 mL) was added to 2,3,4,4a-tetrahydro-1*H*-xanthen-1-one (2.42 g, 10.51mmol) in THF (10 mL) at −78 °C. The mixture was stirred at −78 °C for 15 min. Then, 3-phenyl-2*H*-azirine (0.746 g, 0.636 mmol) in THF (5 mL) was added and the resulting mixture was stirred for 2 h at the same temperature. The reaction was allowed to warm up to room temperature slowly and then stirred for 2 h. The mixture was quenched with water, neutralized with dilute HCl to a pH about 7. The mixture was extracted with CH_2Cl_2 (2 × 50 mL), and the organic layer was washed with brine (2 × 40 mL) and dried over anhydrous $MgSO_4$. After removing the solvents by

evaporation, the resulting crude mixture was separated by column chromatography (*n*-hexane : CH_2Cl_2 = 1 : 1) to afford the pyrrole Opy (1.73 g, 5.26 mmol, 50%) as a pale green solid. HRMS (ESI) m/z calcd for $C_{22}H_{20}NO_2^+$ $(M+H)^+$ 330.14886, found 330.14807.

2.3 Synthesis of OhR-BDP

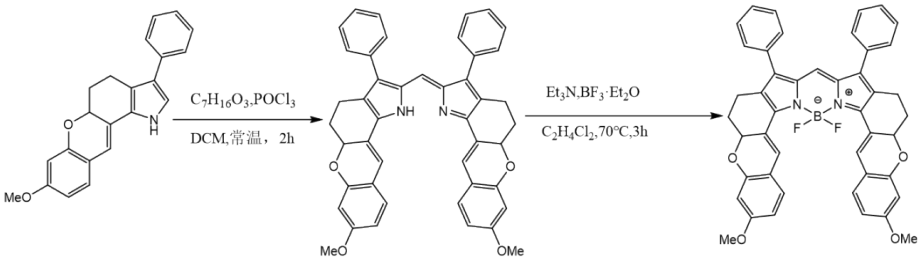

Under N_2, triethyl orthoformate (0.39 g, 0.44 mL, 2.63 mmol) was added to pyrrole Opy in dry DCM (30 mL) and stirred for 10 min, and then $POCl_3$ (0.40 g, 2.63 mmol) was added to the mixture. The reaction was stirred for 2 h at r.t. After evaporation to remove the solvent, the residual mixture was dissolved in anhydrous solvent $ClCH_2CH_2Cl$ (10 mL). Triethylamine (0.5 mL, 3.6 mmol) was added and stirred for 2 h at room temperature, followed by dropwise addition of $BF_3{\cdot}Et_2O$ (1 mL, 8.0 mmol) and stirring for 2 h at 80 °C. After cooling to room temperature, the mixture was extracted with CH_2Cl_2 (2 x 50 ml) and the organic layer was washed with brine (2 x 50 ml) and dried with anhydrous Na_2SO_4. The solvent was removed by evaporation and separated by column chromatography (CH_2Cl_2/*n*-hexane = 2:1) to give OhR-BDP (0.38 g, 0.53 mmol, 20%) as brown solids. Compound OhR-BDP was too insoluble to record a ^{13}C NMR spectrum. ^1H NMR (400 MHz, $CDCl_3$): δ (ppm) 8.21 (s, 1H), 7.27-7.51 (m, 10H), 7.21-7.23 (m, 2H), 6.98 (d, ^3J = 8.0 Hz, 1H), 6.86 (s, 1H), 6.61 (d, ^3J =8.0 Hz, 2H), 6.46 (d, ^4J =2.4 Hz, 2H), 5.11-5.15 (m, 2H), 3.83 (s, 6H), 2.70-2.82 (m, 2H), 2.35-2.48 (m, 2H), 2.03-2.14 (m, 4H). HRMS (ESI) m/z calcd for $C_{45}H_{35}BF_2N_2O_4^+$ $(M+H)^+$ 716.26525, found 716.26563.

2.4 Synthesis of Asy-BDP

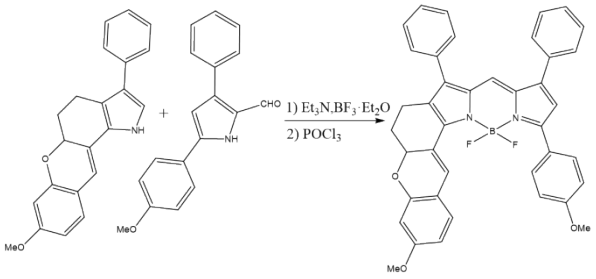

Under N_2, pyrrole Opy (0.48 g, 1.44 mmol) and pyrrole-2-carbaldehyde (0.4 g, 1.44 mmol) was dissolved in 10 mL CH_2Cl_2, and $POCl_3$ (0.22 g, 1.44 mmol) was added dropwise at 0 ºC. The solution was warmed to room temperature slowly and stirred for 6 h. The mixture was cooled to 0 ºC. Et_3N (0.5 mL, 3.58 mmol) was added to the mixture. After stirring for 15 min, $BF_3{\cdot}Et_2O$ (1 mL, 8.0 mmol) was added to the mixture. The mixture was warmed to room temperature and stirred for 6 h. the mixture was washed with water, brine and dried over Na_2SO_4. The solvent was removed under reduced pressure and the residue was purified by column chromatography on silica gel (*n*-hexane : CH_2Cl_2 = 1 : 5), and followed by recrystallization from CH_2Cl_2/*n*-hexane to afford Asy-BDP (0.37 g, 0.58 mmol, 40%) as coppery solids. Compound Asy-BDP was too insoluble to record a ^{13}C NMR spectrum. ^1H NMR (400 MHz, $CDCl_3$): δ (ppm) 8.08 (d, ^3J = 6.4 Hz, 1H), 8.02 (d, ^3J = 8.0 Hz, 2H), 7.39-7.48 (m, 8H), 7.31 (d, ^3J = 8.0 Hz, 2H), 7.11 (d, ^3J = 8.0 Hz, 1H), 7.14 (s, 1H), 7.04 (d, ^3J = 8.0 Hz, 2H), 6.71 (s, 1H), 6.53 (d , ^3J = 8.0 Hz, ^4J = 2.4 Hz, 1H), 6.43 (d, ^4J = 2.4 Hz, 1H), 5.08-5.12 (m, 1H), 3.91 (s, 3H), 3.83 (s, 3H), 2.81-2.85 (m, 2H), 2.63-2.72 (m, 2H). HRMS (ESI) m/z calcd for $C_{40}H_{31}BF_2N_2O_3^+$ $(M)^+$ 636.23903, found 636.23828.

3 NMR

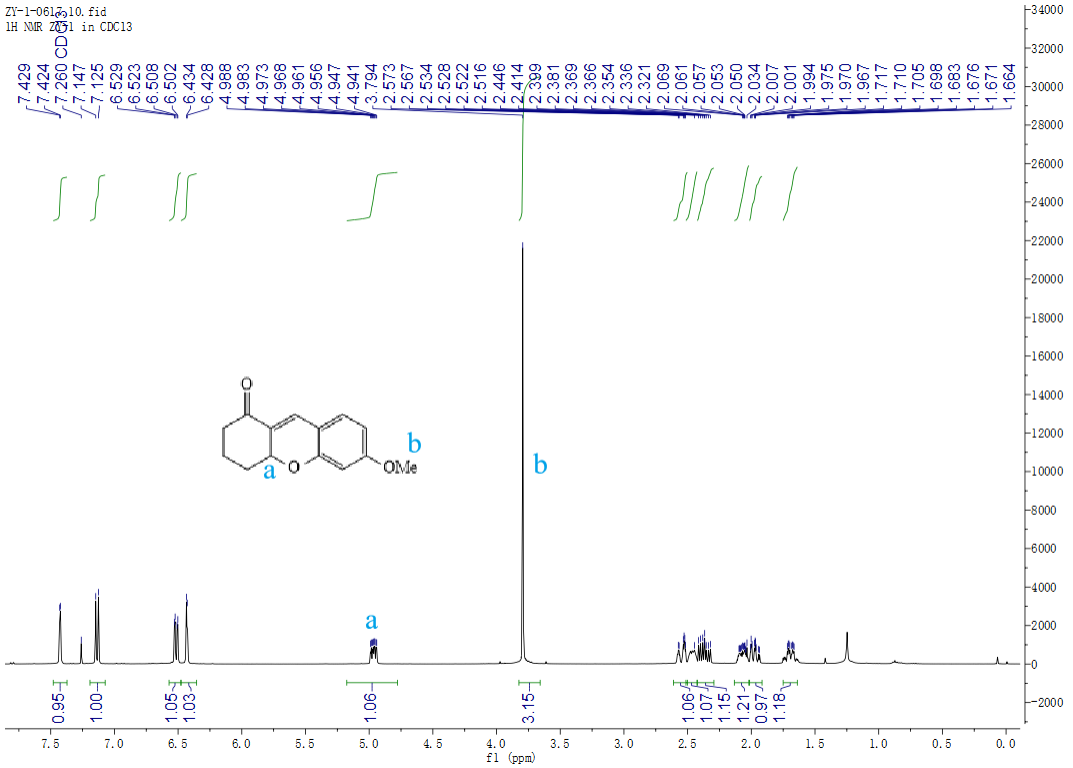
ZY-1-061_10.fid
1H NMR ZY61 in CDCl3
CDCl3
a
b
OMe
f1 (ppm)

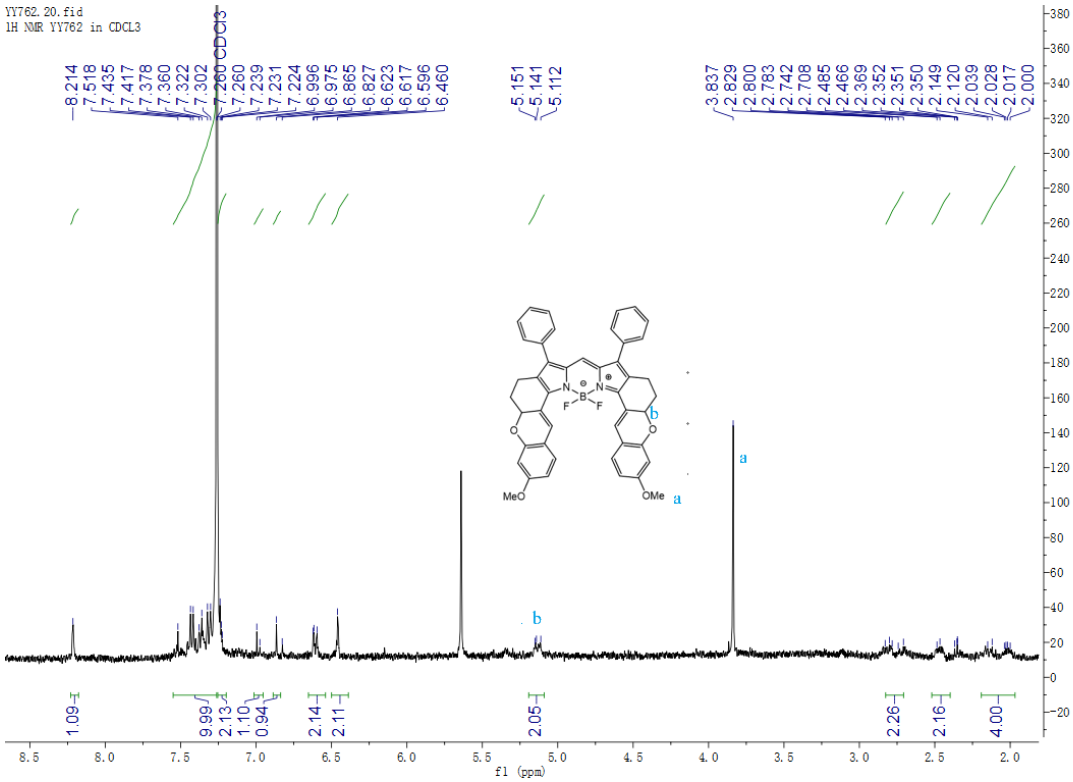
YY762.20.fid
1H NMR YY762 in CDCL3
CDCl3
a
b
MeO
OMe
f1 (ppm)

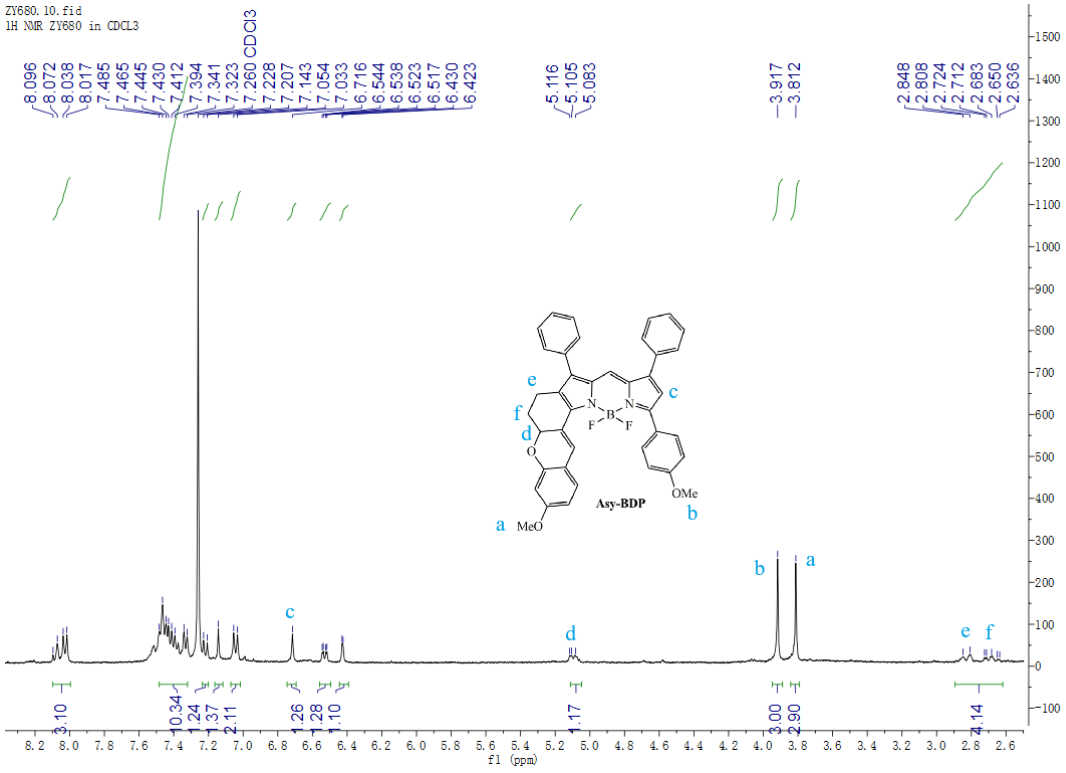
ZY680.10.fid
1H NMR ZY680 in CDCL3
CDCl3
Asy-BDP
MeO
OMe
f1 (ppm)

4 HRMS

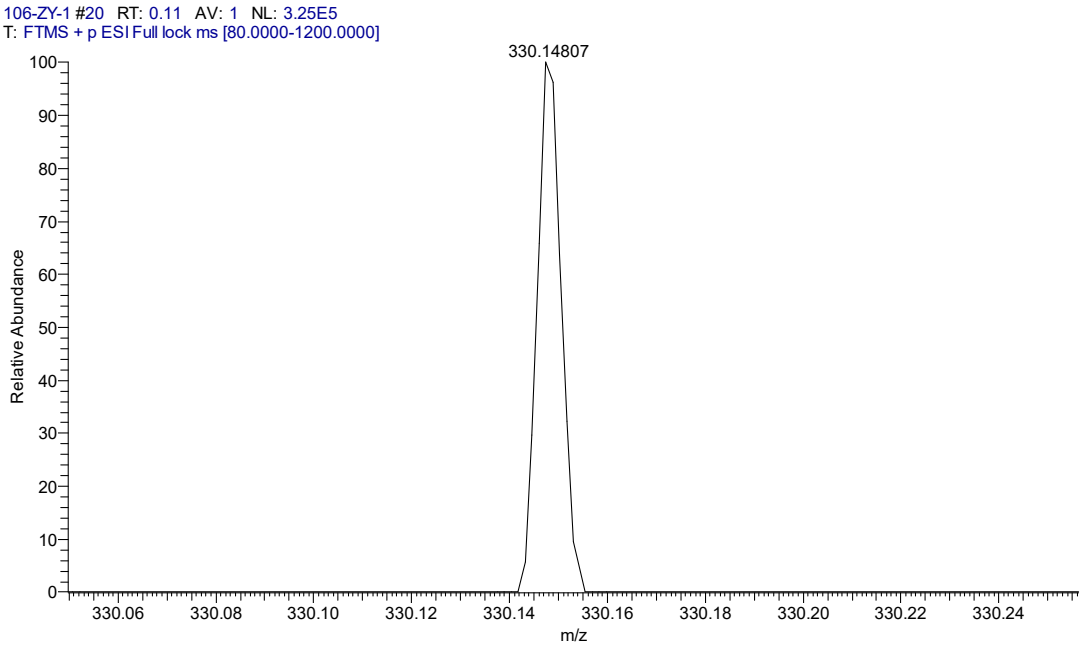

Opy: HRMS (ESI) m/z calcd for $C_{22}H_{20}NO_2^+$ $(M+H)^+$ 330.14886, found 330.14807.

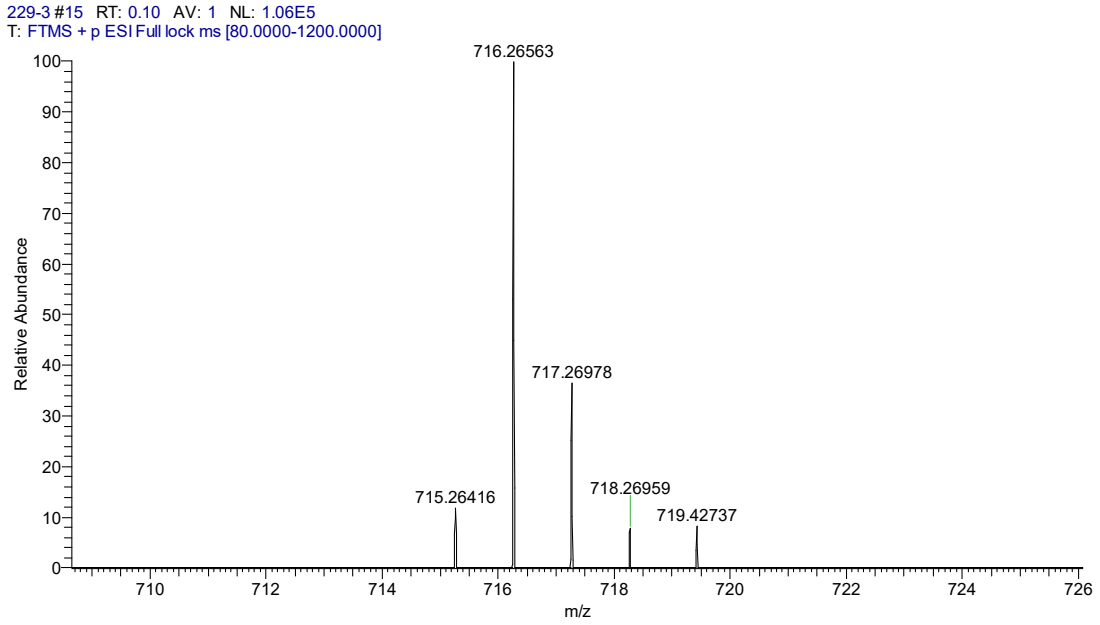

OhR-BDP: HRMS (ESI) m/z calcd for $C_{45}H_{35}BF_2N_2O_4^+$ $(M+H)^+$ 716.26525, found 716.26563.

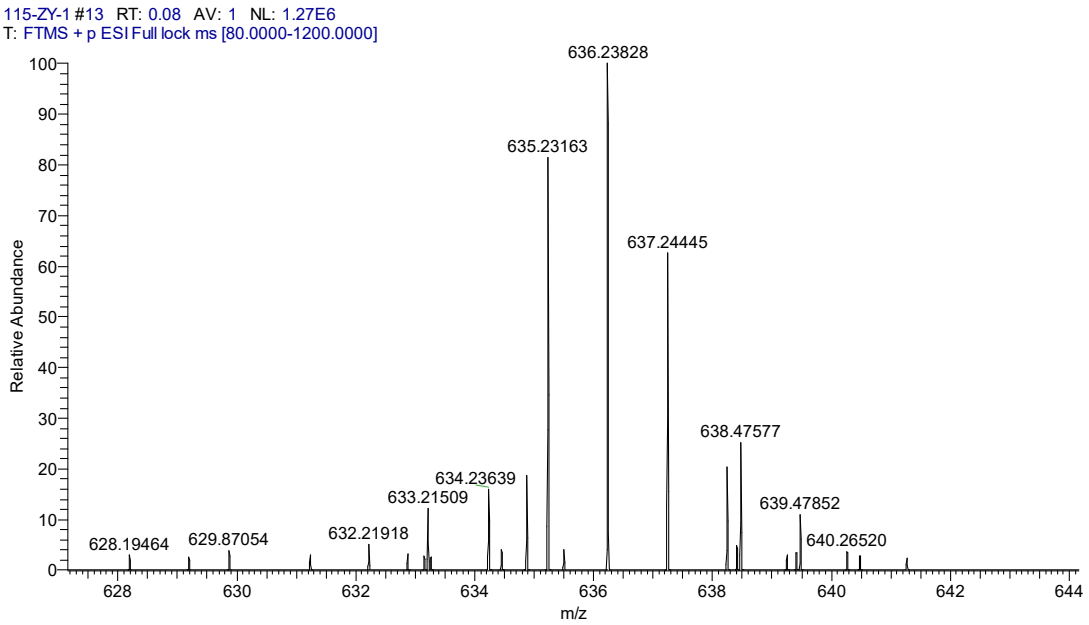

Asy-BDP: HRMS (ESI) m/z calcd for $C_{40}H_{31}BF_2N_2O_3^+$ $(M)^+$ 636.23903, found 636.23828.

5 Figure and Table

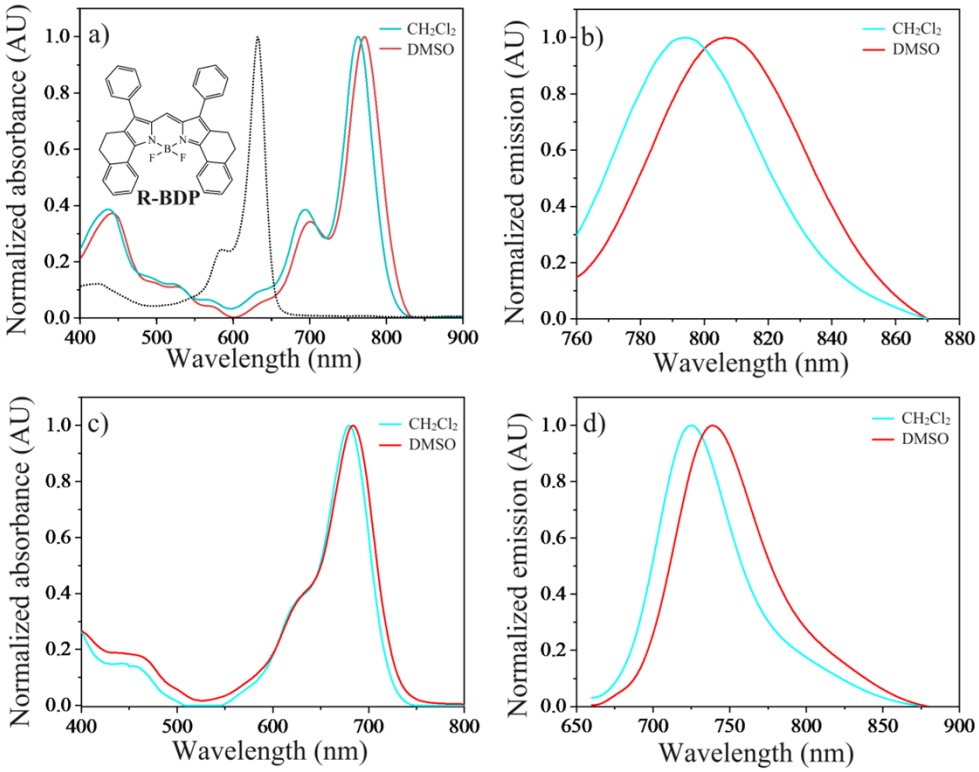

Fig. S1 a) Absorption and b) fluorescence spectra of **OhR-BDP** in CH_2Cl_2 and DMSO at 298 K. c) Absorption and d) fluorescence spectra of **Asy-BDP** in CH_2Cl_2 and DMSO at 298 K.

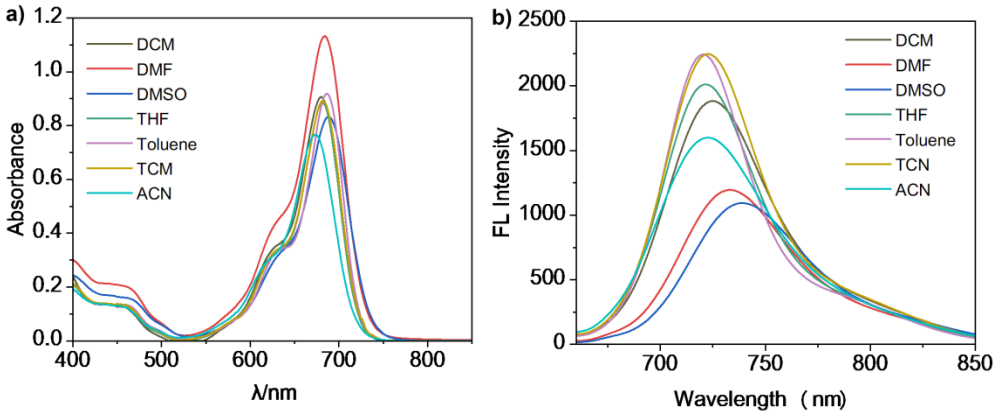

Fig. S2 a) Absorption and b) fluorescence spectra of **Asy-BDP** in different solvents at 298 K.

Table S1 Data of the optical properties of **R-BDP**, **OhR-BDP** and **Asy-BDP** in organic solutions 298 K.

Dye	Solvent	$\lambda_{abs}/\lambda_{em}$ [nm]	Stokes shift [nm]	ε [M^{-1} cm^{-1}]	Φ_f
R-BDP	CH_2Cl_2	632/646	14	123000	0.82
OhR-BDP	CH_2Cl_2	764/794	30	133000	0.04
	DMSO	772/807	50	130000	0.02
Asy-BDP	CH_2Cl_2	680/725	45	126000	0.07
	DMSO	684/739	55	124000	0.05

Herein, we did not build more conformers for either **OhR-BDP** or **Asy-BDP.** We felt confident not to do so for two reasons. The first being the presence of condensed aromatic rings, two in **OhR-BDP** and one in **Asy-BDP**, that we excepted to make the skeletons too rigid and thus prohibit the existence of more than one predominant conformer. The second reason is that since we found only one predominant conformer of **St-BDP** upon changing the orientation of the -OMe groups and we assumed changing the orientations of -OMe in either **OhR-BDP** or **Asy-BDP** would not yield any highly populated conformer.

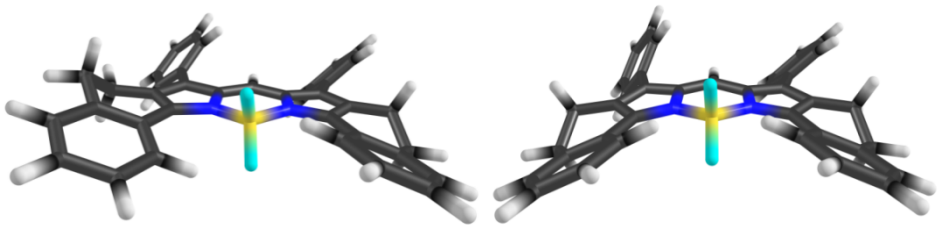

R-BDPa **R-BDPb**

Fig. S3. Two conformers of structure **R-BDP** that were both taken into account for further calculations.

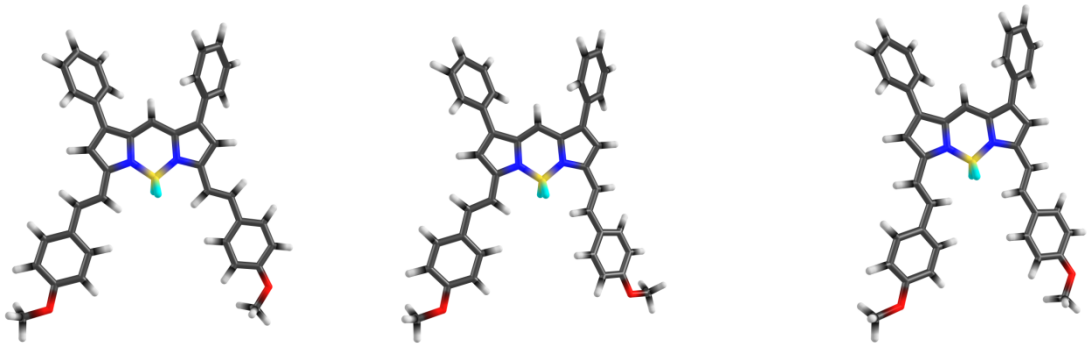

St-BDPa **St-BDPb** **St-BDPc**

Fig. S4. Three conformers of structure **St-BDP**. After geometry optimization only structure **St-BDPa** was taken into account.

Table S2. Gibbs free energies (*G*) and corresponding Boltzman distributions for **St-BDP** and **R-BDP** conformers.

Conformer	Molecule	*G* [eH]	Boltzman distribution %
	St-BDP		
St-BDPa		-1988,6615	99.4
St-BDPb		-1988,6567	0.6
St-BDPc		-1988,6521	0.0
	R-BDP		
R-BDPa		-1759,7381	59.9
R-BDPb		-1759,7378	40.1

Table S3. Charge-transfer computed thanks to Le Bahers' model on the basis of the density difference plots. We report the CT distance representing the eletron-hole separation at the FC point. As well as the amount of transferred charge.

Structure	d_{CT} (Å)	q_{CT} (e)
R-BDPb	0.826	0.398
R-BDPa	0.843	0.395
St-BDP	1.686	0.436
OhR-BDP	1.884	0.474
Asy-BDP	2.077	0.464

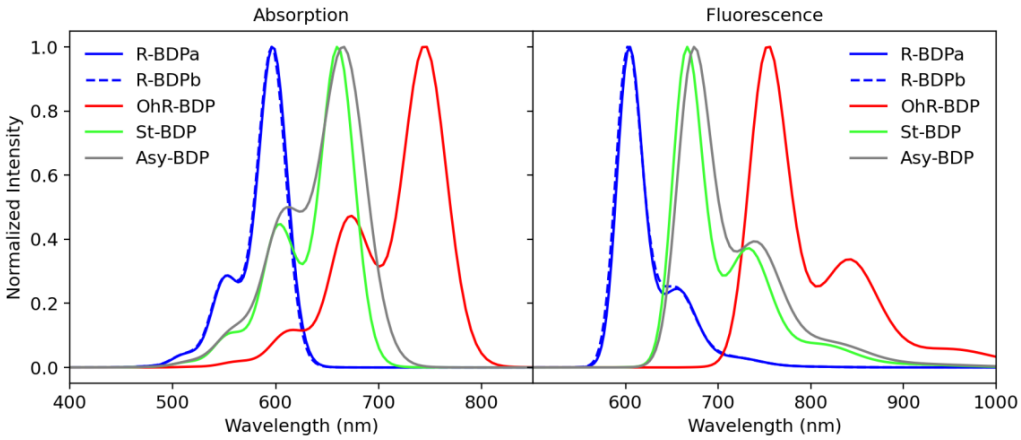

Fig. S5. Theoretical absorption (left) and emission (right) spectra for structures **R-BDPa** (blue full), **R-BDPb** (blue, dashed), **OhR-BDP** (red), **St-BDP** (green) and **Asy-BDP** (gray).

Table S4. Theoretical and experimental $E_{0\text{-}0}$ values in ev and nm for all five strucutres.

	Theoretical		Experimental	
Structure	$E_{0=0}$ [eV]	$E_{0=0}$ [nm]	$E_{0=0}$ [nm]	$E_{0=0}$ [eV]
St-BDP	1.746	710.1	660	1.879
R-BDPa	1.969	629.6	640	1.937
R-BDPb	1.956	633.9	640	1.937
OhR-BDP	1.455	852.4	775	1.600

Table S5. Singlet-triplet gap (in eV) computed on the optimal S_1 geometry and SOC matrix elements (cm^{-1}) determined on the same geometry. The gaps have been computed with three models and the SOC elements have been determined with two models.

	$E_{S\text{-}T}$ (eV) SCS-CC2		$E_{S\text{-}T}$ (eV) CC2		$E_{S\text{-}T}$ (eV) ADC(2)		SOC (cm^{-1}) 1X		SOC (cm^{-1}) 4X	
Structure	S_1-T_1	S_1-T_2	S_1-T_1	S_1-T_2	S_1-T_1	S_1-T_2	S_1-T_1	S_1-T_2	S_1-T_1	S_1-T_2
St-BDP	0.70	-0.41	0.71	-0.37	0.63	-0.46	0.02	0.11	0.02	0.12
R-BDPa	0.67	-0.76	0.69	-0.59	0.60	-0.65	0.05	0.10	0.01	0.06
R-BDPb	0.65	-0.76	0.68	-0.59	0.59	-0.65	0.05	0.06	0.02	0.04
OhR-BDP	0.58	-0.46	0.59	-0.41	0.51	-0.48	0.04	0.20	0.03	0.19
Asy-BDP	0.61	-0.57	0.62	-0.53	0.55	-0.60	0.06	0.23	0.05	0.20

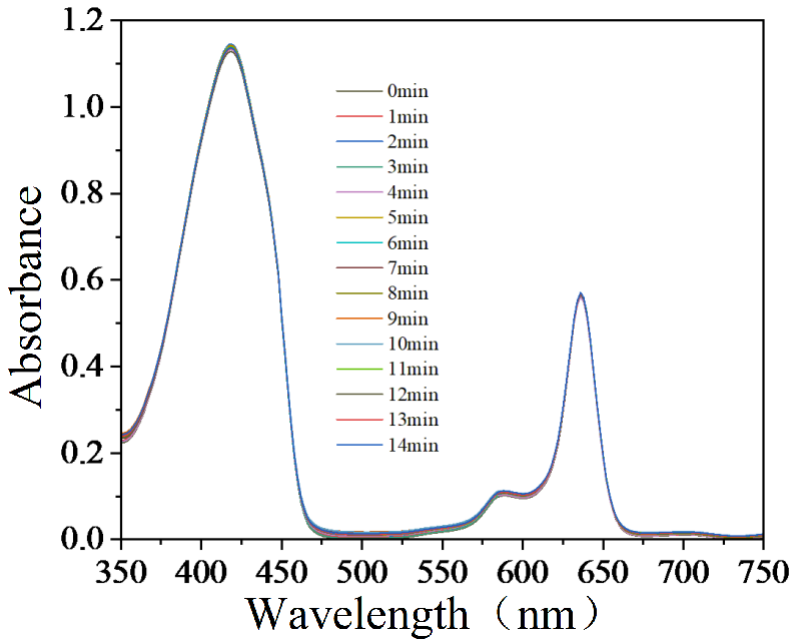

Fig. S6. Time-dependent photo degradation of absorbance at 416 nm by the oxidation of DPBF with **R-azaBDP**. T = 298 K. 635 nm laser.

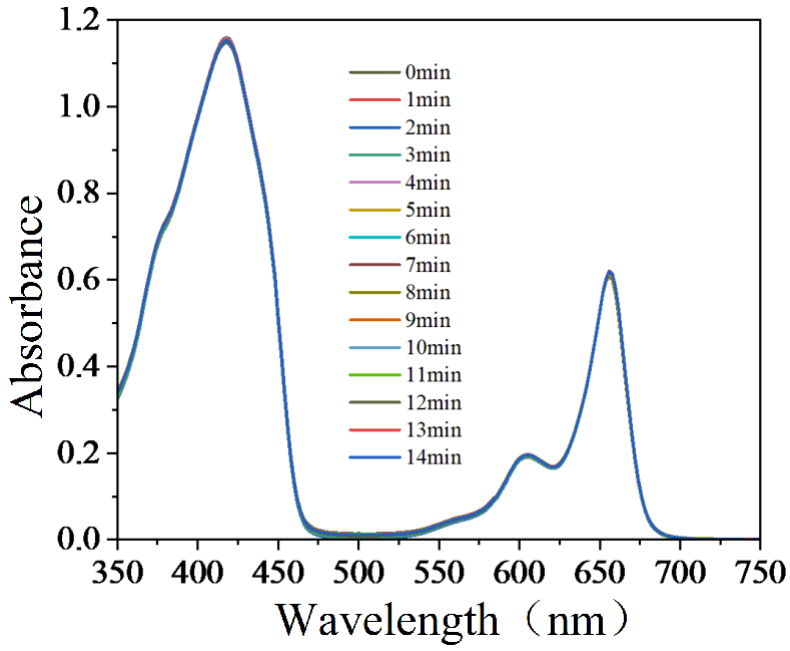

Fig. S7. Time-dependent photo degradation of absorbance at 416 nm by the oxidation of DPBF with **St-azaBDP**. T = 298 K. 635 nm laser.

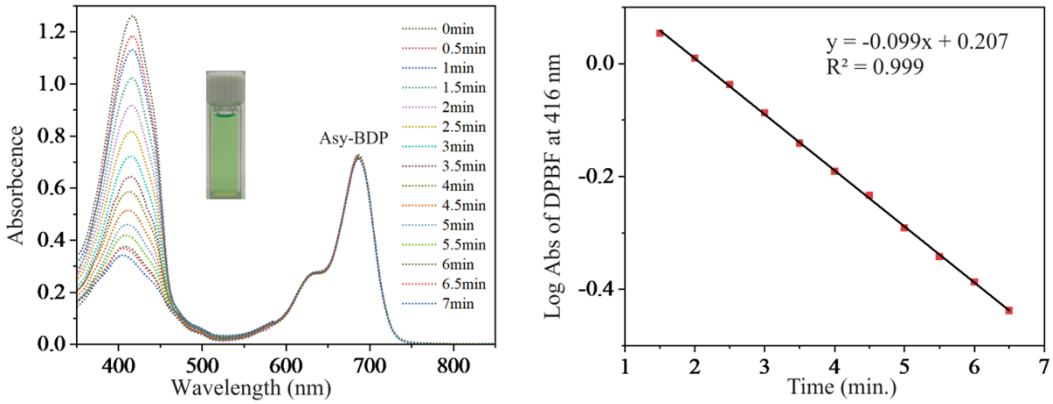

Fig. S8 Time-dependent photo degradation of absorbance at 416 nm by the oxidation of DPBF with a) **Asy-BDP**; b) Comparison of absorption decline rate of DPBF in **Asy-azaBDP** (S = –0.099). T = 298 K. 690 nm laser.

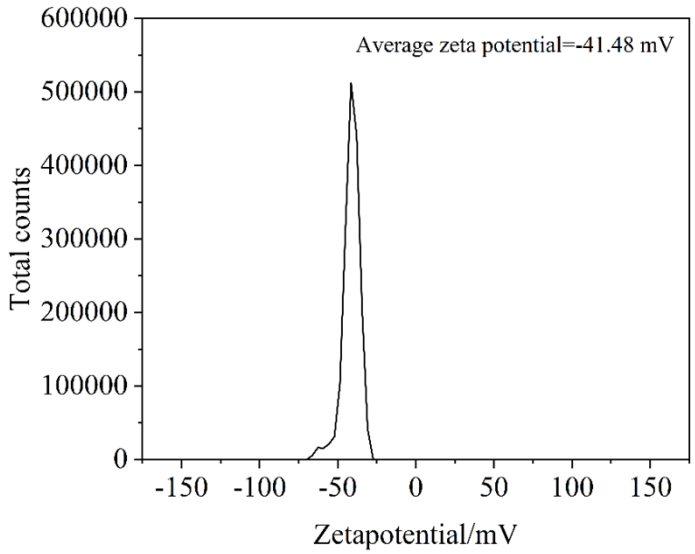

Fig. S9 Zeta potential of **OhR-BDP** NPs

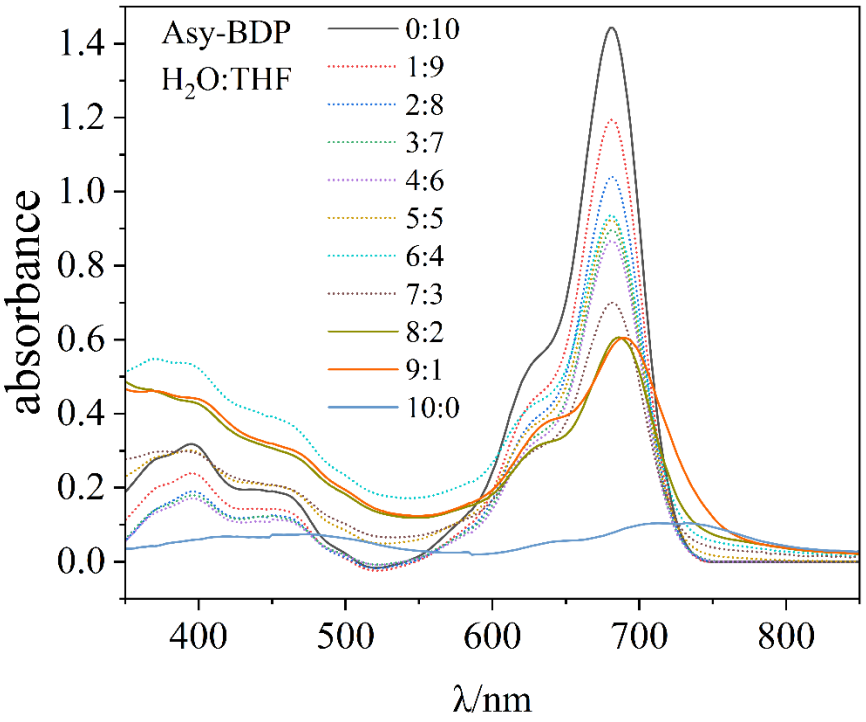

Fig. S10 Absorption spectra of **Asy-BDP** in different proportions of water (0–100%) in THF solution.

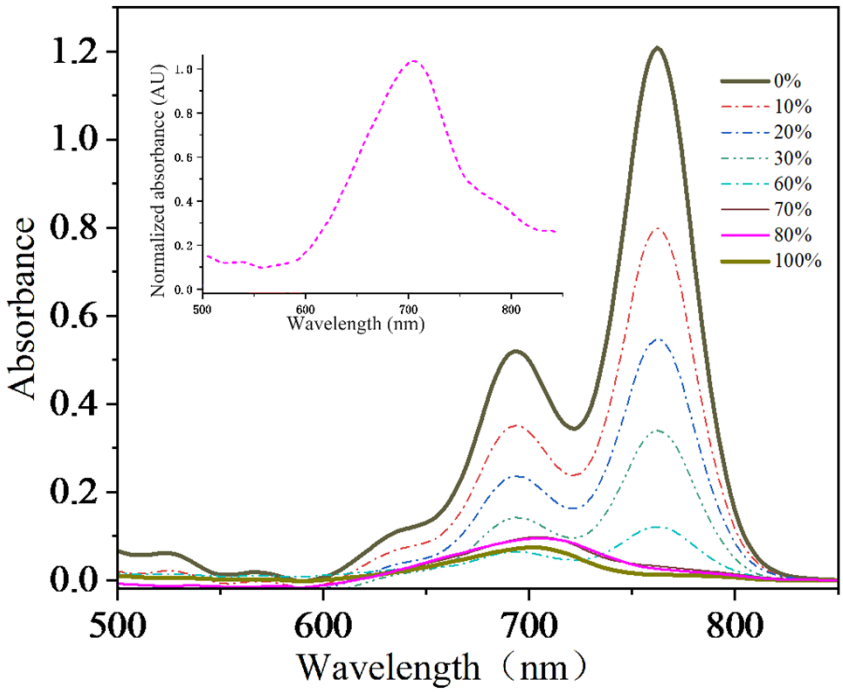

Fig. S11 Absorption spectra of **OhR-BDP** in different proportions of water (0–100%) in THF solution. The inner panel displayed normalized absorption spectra of **OhR-BDP** in H_2O-THF solution (v/v=80:20). When the proportion of water is greater than 70%, *H*-aggregation is formed.

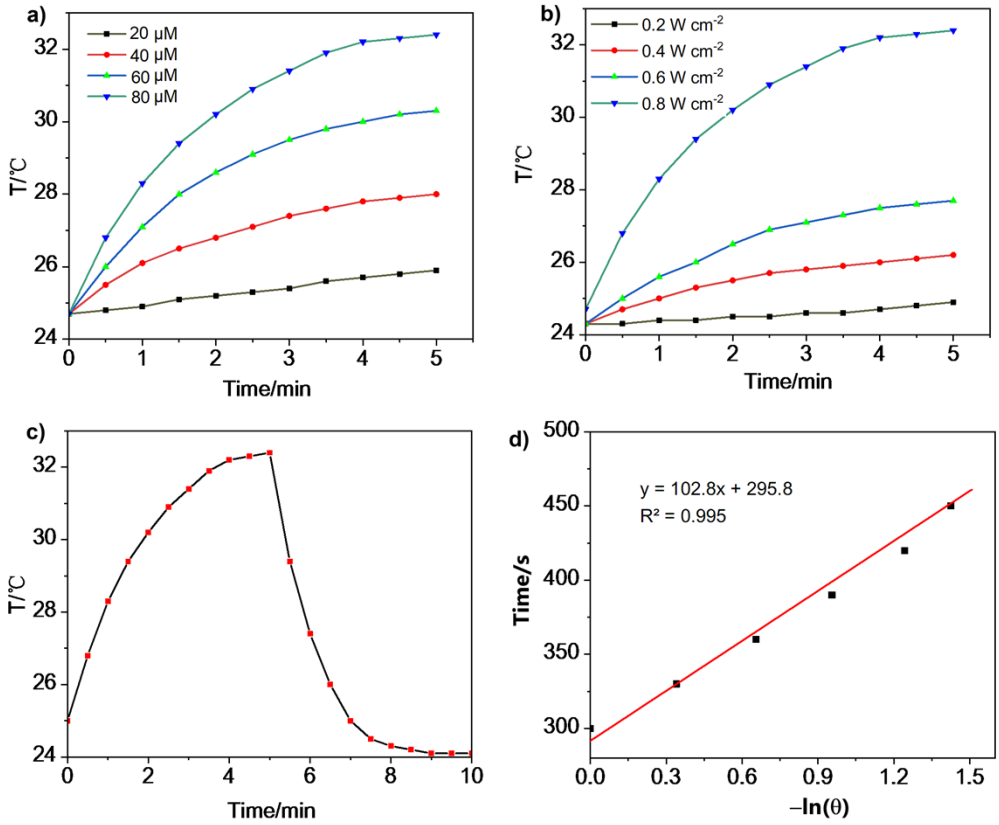

Fig. S12 a) Temperature changes of **OhR-BDP** NPs at different concentrations (20-80 μM) under 808 nm laser irradiation (0.8 W cm^{-2}). b) Photothermal conversion of **OhR-BDP** NPs (80 μM) under 808 nm laser irradiation with different power density (0.2-0.8 W·cm^{-2}). c) Temperature response curves of **OhR-BDP** NPs in aqueous solutions under 808 nm laser irradiation (0.8 W cm^{-2}) and naturally cooling. d) Linear fitting of –ln(θ) and time.

Based on the results of photothermal conversion of **OhR-BDP** NPs, the 40 μM concentration of **OhR-BDP** NPs did not produce the desired temperature difference ($_{\Delta}$T ≈2 °C), and the minimum temperature difference required (42-37) is 5 °C to achieve the effect of PTT in treating tumor cells under 808 nm laser irradiation. So, cell experiments is no longer considered the influence of PTT. Based on the corresponding relationship between cooling time and −Lnθ (Fig. S12d), the photothermal conversion efficiency (η) was calculated as 8.6% under the illumination of 80 μM **OhR-BDP** NPs in aqueous solution.

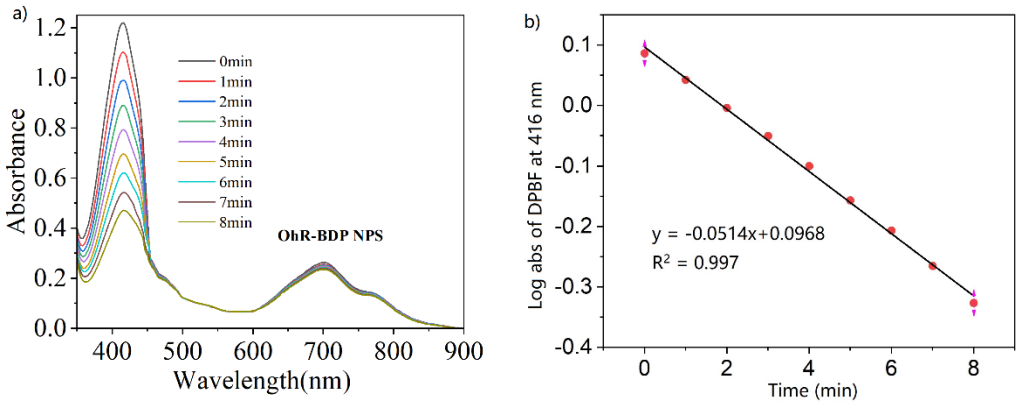

Fig. S13. a) Time-dependent photo degradation of absorbance at 416 nm by the oxidation of DPBF with **OhR-BDP** NPs. T = 298 K. 808nm laser. b) Comparison of absorption decline rate of DPBF in **OhR-BDP** NPs (S = -0.051).

Based on the linear decay curve (Fig. S13), the $^1O_2$ yield of **OhR-BDP** NPs (S = -0.051) was calculated to be 0.36.

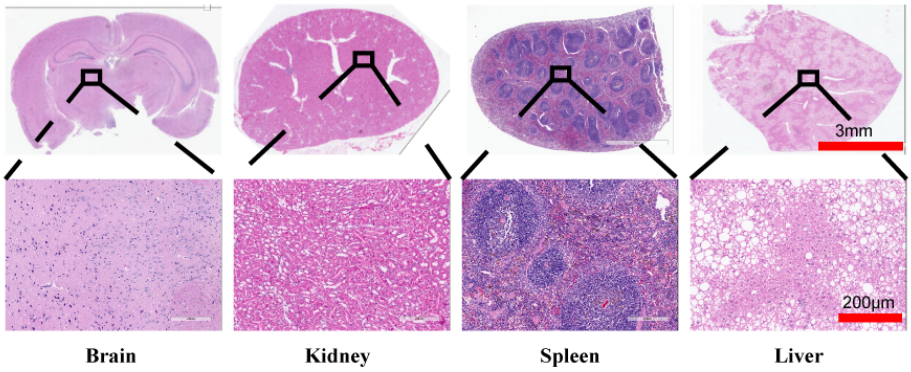

Fig. S14 Biological safety study of OhR-BDP NPs on major organs of mice.

6. X-ray data for Asy-BDP

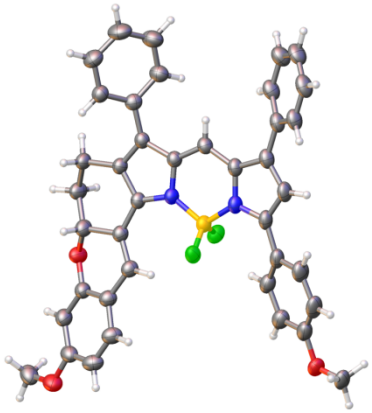

Table 1 Crystal data and structure refinement for zy680.

Identification code	zy680
Empirical formula	$C_{40}H_{31}BF_2N_2O_3$
Formula weight	636.48
Temperature/K	149.98(10)
Crystal system	triclinic
Space group	P-1
a/Å	10.3756(3)
b/Å	11.9998(3)
c/Å	14.3278(4)
α/°	97.047(2)
β/°	105.898(3)
γ/°	96.734(2)
Volume/Å^3	1681.29(8)
Z	2
ρ_{calc}g/cm^3	1.257
μ/mm^{-1}	0.703
F(000)	664.0
Crystal size/mm^3	0.14 × 0.12 × 0.1

Radiation	Cu Kα (λ = 1.54184)
2Θ range for data collection/°	6.5 to 146.93
Index ranges	-12 ≤ h ≤ 10, -14 ≤ k ≤ 14, -17 ≤ l ≤ 17
Reflections collected	20969
Independent reflections	6534 [R_{int} = 0.0512, R_{sigma} = 0.0551]
Data/restraints/parameters	6534/0/459
Goodness-of-fit on F^2	1.060
Final R indexes [I>=2σ (I)]	R_1 = 0.0561, wR_2 = 0.1587
Final R indexes [all data]	R_1 = 0.0676, wR_2 = 0.1704
Largest diff. peak/hole / e $Å^{-3}$	0.43/-0.31

Crystal structure determination of [zy680]

Crystal Data for $C_{40}H_{31}BF_2N_2O_3$ (*M* =636.48 g/mol): triclinic, space group P-1 (no. 2), *a* = 10.3756(3) Å, *b* = 11.9998(3) Å, *c* = 14.3278(4) Å, *α* = 97.047(2)°, *β* = 105.898(3)°, *γ* = 96.734(2)°, *V* = 1681.29(8) $Å^3$, *Z* = 2, *T* = 149.98(10) K, μ(Cu Kα) = 0.703 mm^{-1}, *Dcalc* = 1.257 g/cm^3, 20969 reflections measured (6.5° ≤ 2Θ ≤ 146.93°), 6534 unique (R_{int} = 0.0512, R_{sigma} = 0.0551) which were used in all calculations. The final R_1 was 0.0561 (I > 2σ(I)) and wR_2 was 0.1704 (all data).

Table 2 Fractional Atomic Coordinates ($\times 10^4$) and Equivalent Isotropic Displacement Parameters ($Å^2 \times 10^3$) for zy680. U_{eq} is defined as 1/3 of the trace of the orthogonalised U_{IJ} tensor.

Atom	x	y	z	U(eq)
F1	4861.6(10)	3966.0(8)	3444.8(9)	43.9(3)
F2	6544.9(11)	4815.0(9)	2905.9(8)	45.3(3)
O1	4455.6(14)	8591.5(11)	3665.1(11)	48.0(4)
O2	266.2(15)	8599.7(15)	1221.4(11)	60.3(4)
O3	3001(3)	371(3)	-251(3)	51.7(8)

Table 2 Fractional Atomic Coordinates ($\times 10^4$) and Equivalent Isotropic Displacement Parameters ($Å^2 \times 10^3$) for zy680. U_{eq} is defined as 1/3 of the trace of the orthogonalised U_{IJ} tensor.

Atom	x	y	z	U(eq)
N1	7023.0(15)	3364.1(12)	3943.4(12)	38.9(4)
N2	6689.2(14)	5340.4(12)	4597.6(11)	35.2(3)
C1	7109.1(17)	7024.7(14)	5638.7(14)	36.2(4)
C2	8031.4(17)	6374.8(15)	6079.9(14)	36.4(4)
C3	7777.3(17)	5329.1(15)	5416.1(14)	36.0(4)
C4	8429.7(18)	4393.9(15)	5517.4(14)	38.1(4)
C5	8082.7(18)	3435.4(15)	4795.3(14)	39.4(4)
C6	8543.3(19)	2364.5(16)	4827.3(16)	43.1(4)
C7	9656(2)	2076.9(16)	5597.8(16)	44.4(4)
C8	10833(2)	2847.7(18)	6093.0(17)	48.5(5)
C9	11846(2)	2555(2)	6828.1(19)	56.2(5)
C10	11709(2)	1472(2)	7079.0(19)	57.1(6)
C11	10569(2)	694.8(19)	6579.1(19)	55.5(6)
C12	9551(2)	983.7(17)	5849.9(18)	49.2(5)
C13	7710(2)	1660.7(17)	3990.0(17)	47.8(5)
C14	6782.6(19)	2269.6(16)	3443.1(16)	43.3(4)
C15	5759(2)	1804.6(17)	2501.6(17)	47.2(5)
C16	5190(2)	2434.0(18)	1781.7(16)	48.9(5)
C17	4267(2)	1925(2)	895.9(18)	55.5(5)
C18	3895(2)	750(2)	681.4(19)	57.7(6)
C19	4437(2)	111.5(19)	1376(2)	63.0(7)
C20	5347(2)	625.8(18)	2276(2)	57.3(6)
C21	8983.0(18)	6601.2(15)	7076.6(14)	39.5(4)
C22	10310(2)	6362.9(19)	7269.5(16)	48.9(5)

Table 2 Fractional Atomic Coordinates ($\times 10^4$) and Equivalent Isotropic Displacement Parameters ($Å^2 \times 10^3$) for zy680. U_{eq} is defined as 1/3 of the trace of the orthogonalised U_{IJ} tensor.

Atom	x	y	z	U(eq)
C23	11120(2)	6420(2)	8221.5(18)	59.4(6)
C24	10634(2)	6763(2)	9002.9(18)	64.9(7)
C25	9346(2)	7066(2)	8827.9(16)	53.5(5)
C26	8520(2)	6973.3(16)	7871.9(15)	43.2(4)
C27	6269.3(17)	6377.1(14)	4734.5(13)	35.0(4)
C28	5135.2(18)	6805.2(15)	4131.9(14)	37.8(4)
C29	5008(2)	8028.9(16)	4487.0(15)	45.9(5)
C30	6312(2)	8757.6(17)	5102.2(16)	50.2(5)
C31	6946(2)	8216.9(16)	5988.2(15)	42.3(4)
C32	4090.1(19)	6239.7(16)	3380.0(15)	41.9(4)
C33	3030.0(19)	6821.7(17)	2875.7(15)	43.5(4)
C34	3270.5(19)	8011.8(16)	3029.7(14)	42.5(4)
C35	2383(2)	8639.9(18)	2486.4(15)	48.3(5)
C36	1197(2)	8071(2)	1801.3(15)	48.8(5)
C37	895(2)	6887(2)	1665.8(16)	53.9(5)
C38	1804(2)	6281.7(19)	2189.0(16)	52.0(5)
C39	561(3)	9808(2)	1313.8(18)	60.9(6)
C40	2643(3)	-842(2)	-516(2)	55.2(10)
B1	6234(2)	4375.4(17)	3686.3(16)	37.4(4)
O41	3103(13)	-149(14)	74(10)	78(4)
C	2720(20)	275(17)	-804(18)	82(5)

Table 3 Anisotropic Displacement Parameters ($Å^2 \times 10^3$) for zy680. The Anisotropic displacement factor exponent takes the form: $-2\pi^2[h^2a^{*2}U_{11}+2hka^*b^*U_{12}+\ldots]$.

Atom	U_{11}	U_{22}	U_{33}	U_{23}	U_{13}	U_{12}
F1	41.7(5)	30.3(5)	56.7(7)	-0.7(5)	12.9(5)	5.5(4)
F2	58.8(6)	35.9(5)	40.0(6)	4.1(4)	14.9(5)	4.0(5)
O1	52.8(8)	32.7(7)	50.6(8)	6.1(6)	0.0(6)	12.5(6)
O2	61.2(9)	68.0(10)	47.4(9)	9.6(7)	1.8(7)	26.7(8)
O3	49.8(12)	39.9(14)	56(2)	-9.4(14)	9.1(14)	4.2(10)
N1	43.1(8)	28.8(7)	46.8(9)	3.3(6)	16.9(7)	7.4(6)
N2	39.8(7)	27.0(7)	39.1(8)	4.7(6)	11.2(6)	7.5(6)
C1	39.7(9)	28.4(8)	39.6(10)	3.8(7)	10.8(7)	5.2(7)
C2	36.7(8)	31.0(8)	42.0(10)	5.1(7)	12.8(7)	5.7(7)
C3	37.5(8)	30.8(8)	40.3(10)	5.5(7)	12.0(7)	6.3(7)
C4	41.0(9)	33.5(9)	42.5(10)	9.0(7)	13.7(8)	9.6(7)
C5	44.1(9)	31.3(9)	46.7(11)	6.7(8)	18.3(8)	9.2(7)
C6	47.2(10)	34.0(9)	55.1(12)	10.3(8)	22.6(9)	12.3(8)
C7	48.2(10)	37.2(9)	56.1(12)	10.7(8)	24.0(9)	15.7(8)
C8	49.8(11)	38.8(10)	64.9(13)	17.0(9)	22.8(10)	15.0(8)
C9	49.0(11)	49.3(12)	72.5(15)	14.4(11)	16.8(10)	14.5(9)
C10	58.5(12)	55.7(13)	67.6(15)	22.8(11)	22.4(11)	27.7(10)
C11	62.4(13)	42.5(11)	76.5(16)	22.3(11)	33.5(12)	22.1(10)
C12	53.1(11)	34.8(9)	67.5(14)	10.6(9)	26.3(10)	14.6(8)
C13	52.8(11)	30.5(9)	63.0(13)	2.2(9)	21.6(10)	12.4(8)
C14	47.6(10)	32.0(9)	53.6(12)	-0.4(8)	22.4(9)	8.6(7)
C15	45.4(10)	37.1(10)	59.5(13)	-5.8(9)	22.0(9)	6.0(8)
C16	52.0(11)	41.7(10)	51.6(12)	-4.3(9)	19.1(9)	4.6(8)
C17	51.4(11)	52.2(12)	59.0(13)	-4.9(10)	16.7(10)	5.5(9)
C18	47.1(11)	55.0(13)	65.8(15)	-14.4(11)	18.8(10)	6.9(10)
C19	60.2(13)	37.4(11)	85.5(18)	-16.9(12)	26.7(12)	-0.4(10)
C20	61.3(12)	35.8(10)	73.6(16)	-1.8(10)	21.6(11)	9.5(9)

Table 3 Anisotropic Displacement Parameters ($Å^2×10^3$) for zy680. The Anisotropic displacement factor exponent takes the form: $-2π^2[h^2a^{*2}U_{11}+2hka^*b^*U_{12}+…]$.

C21	42.7(9)	32.4(9)	42.0(10)	8.1(7)	10.6(8)	2.4(7)
C22	42.4(10)	53.2(12)	48.9(12)	9.2(9)	10.1(9)	6.2(8)
C23	43.5(11)	73.3(16)	56.5(14)	11.0(11)	6.6(10)	8.1(10)
C24	58.2(13)	80.1(17)	44.8(12)	10.5(12)	-0.2(10)	1.2(12)
C25	57.6(12)	56.7(13)	41.5(11)	3.2(9)	11.6(9)	2.8(10)
C26	46.4(10)	37.7(9)	44.2(11)	3.6(8)	12.8(8)	5.8(8)
C27	40.0(9)	26.9(8)	38.8(9)	5.0(7)	13.0(7)	5.5(7)
C28	42.5(9)	30.9(8)	39.7(10)	5.9(7)	11.0(8)	6.4(7)
C29	54.7(11)	34.9(10)	44.5(11)	4.8(8)	6.4(9)	14.5(8)
C30	57.5(11)	31.7(9)	52.9(12)	1.8(8)	2.5(10)	12.2(8)
C31	46.8(10)	32.1(9)	43.2(10)	-0.2(8)	6.5(8)	9.4(7)
C32	48.7(10)	33.3(9)	41.1(10)	5.9(8)	9.0(8)	6.5(8)
C33	46.0(10)	40.2(10)	41.1(10)	6.6(8)	7.5(8)	6.2(8)
C34	45.5(10)	40.0(10)	39.9(10)	3.9(8)	7.6(8)	13.1(8)
C35	56.3(11)	42.8(10)	44.1(11)	5.7(9)	8.5(9)	17.2(9)
C36	50.7(11)	59.2(13)	37.8(10)	10.2(9)	9.0(8)	21.2(9)
C37	49.0(11)	60.9(13)	43.5(11)	8.4(10)	2.1(9)	3.1(10)
C38	53.5(11)	45.9(11)	47.9(12)	8.5(9)	2.0(9)	3.4(9)
C39	69.7(14)	68.5(15)	51.2(13)	17.7(11)	14.6(11)	36.3(12)
C40	50.0(15)	40.4(16)	67(2)	-17.2(14)	16.7(14)	1.5(11)
B1	43.2(10)	28.4(9)	41.0(11)	4.7(8)	12.4(9)	7.2(8)
O41	83(7)	73(9)	66(8)	-6(6)	20(6)	-9(6)
C	92(12)	68(10)	78(12)	0(10)	15(10)	22(8)

Table 4 Bond Lengths for zy680.

Atom	Atom	Length/Å	Atom	Atom	Length/Å
F1	B1	1.383(2)	C11	C12	1.378(3)
F2	B1	1.391(2)	C13	C14	1.402(3)
O1	C29	1.445(2)	C14	C15	1.467(3)
O1	C34	1.362(2)	C15	C16	1.394(3)
O2	C36	1.363(3)	C15	C20	1.399(3)
O2	C39	1.429(3)	C16	C17	1.381(3)
O3	C18	1.387(4)	C17	C18	1.390(3)
O3	C40	1.435(4)	C18	C19	1.370(4)
N1	C5	1.387(3)	C18	O41	1.330(12)
N1	C14	1.377(2)	C19	C20	1.391(4)
N1	B1	1.567(3)	C21	C22	1.399(3)
N2	C3	1.390(2)	C21	C26	1.398(3)
N2	C27	1.375(2)	C22	C23	1.381(3)
N2	B1	1.559(2)	C23	C24	1.386(4)
C1	C2	1.374(3)	C24	C25	1.391(4)
C1	C27	1.420(3)	C25	C26	1.386(3)
C1	C31	1.501(2)	C27	C28	1.445(3)
C2	C3	1.429(2)	C28	C29	1.527(3)
C2	C21	1.469(3)	C28	C32	1.343(3)
C3	C4	1.379(3)	C29	C30	1.501(3)
C4	C5	1.389(3)	C30	C31	1.520(3)
C5	C6	1.424(3)	C32	C33	1.445(3)
C6	C7	1.469(3)	C33	C34	1.400(3)
C6	C13	1.383(3)	C33	C38	1.404(3)
C7	C8	1.396(3)	C34	C35	1.392(3)
C7	C12	1.403(3)	C35	C36	1.386(3)
C8	C9	1.382(3)	C36	C37	1.396(3)

Table 4 Bond Lengths for zy680.

C9	C10	1.392(3)	C37	C38	1.373(3)
C10	C11	1.376(4)	O41	C	1.39(3)

Table 5 Bond Angles for zy680.

Atom	Atom	Atom	Angle/°	Atom	Atom	Atom	Angle/°
C34	O1	C29	113.76(15)	C19	C18	C17	118.6(2)
C36	O2	C39	117.45(17)	O41	C18	C17	148.1(8)
C18	O3	C40	115.1(3)	O41	C18	C19	93.0(8)
C5	N1	B1	123.12(15)	C18	C19	C20	120.8(2)
C14	N1	C5	107.88(16)	C19	C20	C15	121.7(2)
C14	N1	B1	128.89(16)	C22	C21	C2	122.14(18)
C3	N2	B1	122.87(14)	C26	C21	C2	119.17(17)
C27	N2	C3	106.52(14)	C26	C21	C22	118.44(18)
C27	N2	B1	130.22(15)	C23	C22	C21	121.1(2)
C2	C1	C27	108.29(15)	C22	C23	C24	119.7(2)
C2	C1	C31	129.14(16)	C23	C24	C25	120.1(2)
C27	C1	C31	122.57(16)	C26	C25	C24	120.1(2)
C1	C2	C3	106.06(16)	C25	C26	C21	120.44(19)
C1	C2	C21	128.84(16)	N2	C27	C1	109.29(15)
C3	C2	C21	124.68(16)	N2	C27	C28	129.36(16)
N2	C3	C2	109.80(15)	C1	C27	C28	121.28(16)
C4	C3	N2	121.39(16)	C27	C28	C29	115.15(15)
C4	C3	C2	128.80(17)	C32	C28	C27	129.00(17)
C3	C4	C5	122.33(18)	C32	C28	C29	115.28(17)
N1	C5	C4	120.93(16)	O1	C29	C28	110.83(16)
N1	C5	C6	109.23(16)	O1	C29	C30	107.25(17)

Table 5 Bond Angles for zy680.

Atom	Atom	Atom	Angle/°	Atom	Atom	Atom	Angle/°
C4	C5	C6	129.27(19)	C30	C29	C28	114.85(16)
C5	C6	C7	126.88(19)	C29	C30	C31	110.04(17)
C13	C6	C5	105.25(17)	C1	C31	C30	108.96(16)
C13	C6	C7	127.86(18)	C28	C32	C33	120.71(18)
C8	C7	C6	122.72(18)	C34	C33	C32	118.04(17)
C8	C7	C12	117.91(19)	C34	C33	C38	117.05(18)
C12	C7	C6	119.37(19)	C38	C33	C32	124.77(19)
C9	C8	C7	121.13(19)	O1	C34	C33	120.23(17)
C8	C9	C10	119.9(2)	O1	C34	C35	117.54(18)
C11	C10	C9	119.5(2)	C35	C34	C33	121.99(18)
C10	C11	C12	120.8(2)	C36	C35	C34	118.97(19)
C11	C12	C7	120.7(2)	O2	C36	C35	123.9(2)
C6	C13	C14	109.84(17)	O2	C36	C37	115.75(19)
N1	C14	C13	107.77(17)	C35	C36	C37	120.39(19)
N1	C14	C15	127.09(18)	C38	C37	C36	119.67(19)
C13	C14	C15	125.13(17)	C37	C38	C33	121.8(2)
C16	C15	C14	125.53(18)	F1	B1	F2	110.56(16)
C16	C15	C20	116.3(2)	F1	B1	N1	107.75(14)
C20	C15	C14	118.1(2)	F1	B1	N2	111.53(15)
C17	C16	C15	122.0(2)	F2	B1	N1	110.52(15)
C16	C17	C18	120.6(2)	F2	B1	N2	107.88(14)
O3	C18	C17	113.5(3)	N2	B1	N1	108.60(15)
C19	C18	O3	127.9(2)	C18	O41	C	101.9(14)

Table 6 Torsion Angles for zy680.

A	B	C	D	Angle/°	A	B	C	D	Angle/°

Table 6 Torsion Angles for zy680.

A	B	C	D	Angle/°	A	B	C	D	Angle/°
O1	C29	C30	C31	179.62(16)	C16	C17	C18	O3	-177.6(2)
O1	C34	C35	C36	177.11(19)	C16	C17	C18	C19	1.6(3)
O2	C36	C37	C38	177.2(2)	C16	C17	C18	O41	173.7(10)
O3	C18	C19	C20	178.7(2)	C17	C18	C19	C20	-0.4(3)
N1	C5	C6	C7	179.36(17)	C17	C18	O41	C	22.2(19)
N1	C5	C6	C13	-1.4(2)	C18	C19	C20	C15	-0.9(4)
N1	C14	C15	C16	24.6(3)	C19	C18	O41	C	-164.7(12)
N1	C14	C15	C20	-158.3(2)	C20	C15	C16	C17	0.3(3)
N2	C3	C4	C5	2.9(3)	C21	C2	C3	N2	171.48(16)
N2	C27	C28	C29	-177.33(18)	C21	C2	C3	C4	-6.9(3)
N2	C27	C28	C32	11.9(3)	C21	C22	C23	C24	-2.6(4)
C1	C2	C3	N2	-1.6(2)	C22	C21	C26	C25	-2.1(3)
C1	C2	C3	C4	179.98(18)	C22	C23	C24	C25	-1.1(4)
C1	C2	C21	C22	-139.9(2)	C23	C24	C25	C26	3.2(4)
C1	C2	C21	C26	45.8(3)	C24	C25	C26	C21	-1.6(3)
C1	C27	C28	C29	5.9(3)	C26	C21	C22	C23	4.2(3)
C1	C27	C28	C32	-164.91(19)	C27	N2	C3	C2	0.57(19)
C2	C1	C27	N2	-1.7(2)	C27	N2	C3	C4	179.11(17)
C2	C1	C27	C28	175.65(16)	C27	N2	B1	F1	-60.1(2)
C2	C1	C31	C30	153.2(2)	C27	N2	B1	F2	61.5(2)
C2	C3	C4	C5	-178.85(18)	C27	N2	B1	N1	-178.65(16)
C2	C21	C22	C23	-170.1(2)	C27	C1	C2	C3	2.0(2)
C2	C21	C26	C25	172.44(18)	C27	C1	C2	C21	-170.73(17)
C3	N2	C27	C1	0.67(19)	C27	C1	C31	C30	-26.2(2)
C3	N2	C27	C28	-176.41(18)	C27	C28	C29	O1	146.95(16)
C3	N2	B1	F1	128.09(17)	C27	C28	C29	C30	25.2(3)

Table 6 Torsion Angles for zy680.

A	B	C	D	Angle/°	A	B	C	D	Angle/°
C3	N2	B1	F2	-110.31(18)	C27	C28	C32	C33	178.78(19)
C3	N2	B1	N1	9.5(2)	C28	C29	C30	C31	-56.7(2)
C3	C2	C21	C22	48.6(3)	C28	C32	C33	C34	14.6(3)
C3	C2	C21	C26	-125.6(2)	C28	C32	C33	C38	-169.8(2)
C3	C4	C5	N1	-2.0(3)	C29	O1	C34	C33	-32.3(3)
C3	C4	C5	C6	-172.34(19)	C29	O1	C34	C35	153.20(18)
C4	C5	C6	C7	-9.4(3)	C29	C28	C32	C33	8.0(3)
C4	C5	C6	C13	169.80(19)	C29	C30	C31	C1	54.9(2)
C5	N1	C14	C13	-0.3(2)	C31	C1	C2	C3	-177.54(18)
C5	N1	C14	C15	-179.71(18)	C31	C1	C2	C21	9.8(3)
C5	N1	B1	F1	-129.62(17)	C31	C1	C27	N2	177.84(16)
C5	N1	B1	F2	109.48(19)	C31	C1	C27	C28	-4.8(3)
C5	N1	B1	N2	-8.7(2)	C32	C28	C29	O1	-40.9(2)
C5	C6	C7	C8	-35.7(3)	C32	C28	C29	C30	-162.67(19)
C5	C6	C7	C12	144.8(2)	C32	C33	C34	O1	-2.2(3)
C5	C6	C13	C14	1.2(2)	C32	C33	C34	C35	171.96(19)
C6	C7	C8	C9	178.6(2)	C32	C33	C38	C37	-173.6(2)
C6	C7	C12	C11	-179.06(19)	C33	C34	C35	C36	2.8(3)
C6	C13	C14	N1	-0.6(2)	C34	O1	C29	C28	52.9(2)
C6	C13	C14	C15	178.81(18)	C34	O1	C29	C30	179.00(16)
C7	C6	C13	C14	-179.58(18)	C34	C33	C38	C37	2.0(3)
C7	C8	C9	C10	0.7(4)	C34	C35	C36	O2	-179.10(19)
C8	C7	C12	C11	1.4(3)	C34	C35	C36	C37	0.5(3)
C8	C9	C10	C11	1.0(4)	C35	C36	C37	C38	-2.5(3)
C9	C10	C11	C12	-1.5(4)	C36	C37	C38	C33	1.1(4)
C10	C11	C12	C7	0.2(3)	C38	C33	C34	O1	-178.18(19)

Table 6 Torsion Angles for zy680.

A	B	C	D	Angle/°	A	B	C	D	Angle/°
C12	C7	C8	C9	-1.9(3)	C38	C33	C34	C35	-4.0(3)
C13	C6	C7	C8	145.3(2)	C39	O2	C36	C35	1.8(3)
C13	C6	C7	C12	-34.3(3)	C39	O2	C36	C37	-177.9(2)
C13	C14	C15	C16	-154.6(2)	C40	O3	C18	C17	177.2(2)
C13	C14	C15	C20	22.5(3)	C40	O3	C18	C19	-1.9(4)
C14	N1	C5	C4	-170.97(17)	B1	N1	C5	C4	5.6(3)
C14	N1	C5	C6	1.1(2)	B1	N1	C5	C6	177.67(16)
C14	N1	B1	F1	46.2(3)	B1	N1	C14	C13	-176.66(18)
C14	N1	B1	F2	-74.7(2)	B1	N1	C14	C15	4.0(3)
C14	N1	B1	N2	167.13(17)	B1	N2	C3	C2	174.09(15)
C14	C15	C16	C17	177.44(19)	B1	N2	C3	C4	-7.4(3)
C14	C15	C20	C19	-176.45(19)	B1	N2	C27	C1	-172.19(17)
C15	C16	C17	C18	-1.6(3)	B1	N2	C27	C28	10.7(3)
C16	C15	C20	C19	0.9(3)	O41	C18	C19	C20	-176.2(6)

Table 7 Hydrogen Atom Coordinates (Å×10^4) and Isotropic Displacement Parameters (Å^2×10^3) for zy680.

Atom	x	y	z	U(eq)
H4	9141.63	4405.78	6101.72	46
H8	10938.93	3585.85	5921.39	58
H9	12636.43	3092.74	7162.26	67
H10	12395.92	1270.68	7591.15	69
H11	10483.52	-50.28	6739.02	67
H12	8770.29	437.04	5514.29	59
H13	7759.02	881.05	3811.8	57
H16	5445.42	3236.9	1904.17	59

Table 7 Hydrogen Atom Coordinates (Å×10^4) and Isotropic Displacement Parameters (Å^2×10^3) for zy680.

Atom	x	y	z	U(eq)
H17	3883.19	2381.77	428.86	67
H19	4187.52	-692.1	1242.52	76
H20	5698.56	164.93	2749.31	69
H22	10660.42	6158.5	6736.39	59
H23	12005.67	6224.59	8340.25	71
H24	11181.87	6790.11	9658.84	78
H25	9033.29	7338.14	9364.24	64
H26	7632.14	7163.56	7756.19	52
H29	4360.69	8005.3	4891.52	55
H30A	6133.8	9522.62	5326.01	60
H30B	6949.07	8844.81	4702.86	60
H31A	7842.35	8665	6362.67	51
H31B	6358.12	8206.37	6427.83	51
H32	4030(20)	5450(20)	3160(18)	56(7)
H35	2586.37	9445.94	2583.79	58
H37	64.39	6501.94	1213.93	65
H38	1597.16	5475.47	2083.36	62
H39A	-164.58	10079.4	843.27	91
H39B	1425.61	10018.31	1177.95	91
H39C	624.94	10156.66	1983.66	91
H40A	2023.78	-1031.56	-1185.69	83
H40B	2196.01	-1140.15	-57.42	83
H40C	3465.1	-1180.98	-484.93	83
HA	2182.09	-340.02	-1330.91	123
HB	3528.21	590.14	-966.73	123

Table 7 Hydrogen Atom Coordinates (Å×10^4) and Isotropic Displacement Parameters (Å^2×10^3) for zy680.

Atom	x	y	z	U(eq)
HC	2168.63	874.06	-733.31	123

Table 8 Atomic Occupancy for zy680.

Atom	Occupancy	Atom	Occupancy	Atom	Occupancy
O3	0.793(8)	C40	0.793(8)	H40A	0.793(8)
H40B	0.793(8)	H40C	0.793(8)	O41	0.207(8)
C	0.207(8)	HA	0.207(8)	HB	0.207(8)
HC	0.207(8)				

Table 9 Solvent masks information for zy680.

Number	X	Y	Z	Volume	Electron count	Content
1	0.513	0.500	0.000	238.8	60.3	?

Experimental

Single crystals of $C_{40}H_{31}BF_2N_2O_3$ **[zy680]** were **[]**. A suitable crystal was selected and **[]** on a **XtaLAB Synergy R, DW system, HyPix** diffractometer. The crystal was kept at 149.98(10) K during data collection. Using Olex2 [1], the structure was solved with the Unknown [2] structure solution program using Unknown and refined with the Unknown [3] refinement package using Unknown minimisation.

7 Checkcif

checkCIF/PLATON report

Structure factors have been supplied for datablock(s) zy680

THIS REPORT IS FOR GUIDANCE ONLY. IF USED AS PART OF A REVIEW PROCEDURE FOR PUBLICATION, IT SHOULD NOT REPLACE THE EXPERTISE OF AN EXPERIENCED CRYSTALLOGRAPHIC REFEREE.

No syntax errors found. CIF dictionary Interpreting this report

Datablock: zy680

Bond precision: C-C = 0.0030 A Wavelength=1.54184

Cell: a=10.3756(3) b=11.9998(3) c=14.3278(4)
alpha=97.047(2) beta=105.898(3) gamma=96.734(2)
Temperature: 150 K

	Calculated	Reported
Volume	1681.29(9)	1681.29(8)
Space group	P -1	P -1
Hall group	-P 1	-P 1
Moiety formula	C40 H31 B F2 N2 O3 [+ solvent]	C40 H31 B F2 N2 O3
Sum formula	C40 H31 B F2 N2 O3 [+ solvent]	C40 H31 B F2 N2 O3
Mr	636.48	636.48
Dx,g cm-3	1.257	1.257
Z	2	2
Mu (mm-1)	0.703	0.703
F000	664.0	664.0
F000'	666.08	
h,k,lmax	12,14,17	12,14,17
Nref	6755	6534
Tmin,Tmax	0.906,0.932	0.762,1.000
Tmin'	0.906	

Correction method= # Reported T Limits: Tmin=0.762 Tmax=1.000
AbsCorr = MULTI-SCAN

Data completeness= 0.967 Theta(max)= 73.465

R(reflections)= 0.0561(5103)

wR2(reflections)= 0.1704(6534)

S = 1.060 Npar= 459

The following ALERTS were generated. Each ALERT has the format
test-name_ALERT_alert-type_alert-level.
Click on the hyperlinks for more details of the test.

Alert level C

```
PLAT230_ALERT_2_C Hirshfeld Test Diff for    C18      --C19      .        5.9 s.u.
PLAT911_ALERT_3_C Missing FCF Refl Between Thmin & STh/L=    0.600         20 Report
              -12  0  1, -12 -1  2,  -2-13  3, -12 -1  3,  11  0  3, -12  5  3,
              -12 -2  4,   9  5  4, -12 -2  5,   1 -2  5,   8  5  5, -12 -2  6,
                7  6  6,   8 -7  8,   5  7  8, -11 -2  9,   7 -3 11,  -9  3 13,
               -1 -3 14,  -7  3 15,
```

Alert level G

```
PLAT072_ALERT_2_G SHELXL First  Parameter in WGHT  Unusually Large       0.10 Report
PLAT230_ALERT_2_G Hirshfeld Test Diff for    O3       --C18      .        5.5 s.u.
PLAT301_ALERT_3_G Main Residue  Disorder ..............(Resd    1)         4% Note
PLAT398_ALERT_2_G Deviating  C-O-C   Angle From 120 for O41      .      101.9 Degree
PLAT432_ALERT_2_G Short Inter X...Y Contact  F1       ..C1       .       2.93 Ang.
                                          1-x,1-y,1-z  =      2_666 Check
PLAT605_ALERT_4_G Largest Solvent Accessible VOID in the Structure       218 A**3
PLAT720_ALERT_4_G Number of Unusual/Non-Standard Labels ..........         3 Note
              Ha      Hb      Hc
PLAT868_ALERT_4_G ALERTS Due to the Use of _smtbx_masks Suppressed         ! Info
PLAT912_ALERT_4_G Missing # of FCF Reflections Above STh/L=  0.600       201 Note
PLAT941_ALERT_3_G Average HKL Measurement Multiplicity ...........       3.2 Low
PLAT969_ALERT_5_G The 'Henn et al.' R-Factor-gap value ...........      2.39 Note
              Predicted wR2: Based on SigI**2  7.12 or SHELX Weight 16.66
PLAT978_ALERT_2_G Number C-C Bonds with Positive Residual Density.         4 Info
```

```
   0 ALERT level A = Most likely a serious problem - resolve or explain
   0 ALERT level B = A potentially serious problem, consider carefully
   2 ALERT level C = Check. Ensure it is not caused by an omission or oversight
  12 ALERT level G = General information/check it is not something unexpected

   0 ALERT type 1 CIF construction/syntax error, inconsistent or missing data
   6 ALERT type 2 Indicator that the structure model may be wrong or deficient
   3 ALERT type 3 Indicator that the structure quality may be low
   4 ALERT type 4 Improvement, methodology, query or suggestion
   1 ALERT type 5 Informative message, check
```

Datablock zy680 - ellipsoid plot